![frontiers logo] Frontiers in Materials

Programmable Manipulations of Terahertz Beams by Graphene-Based Metasurface With Both Amplitude and Phase Modulations

Chenxi Liu, Fei Yang *, Xiaojian Fu, Junwei Wu and Lei Zhang

State Key Laboratory of Millimeter Waves, School of Information Science and Engineering, Southeast University, Nanjing, China

Terahertz metasurface with digital, programmable control recently gained considerable attention for its potential applications in high-speed imaging, nondestructive sensing, and wireless communication. With elaborate design, the metasurface can perform amplitude, phase, and polarization modulations of electromagnetic waves. Most digital programmable metasurfaces focus on only one of the three dimensions. Here, we propose a graphene-based THz metasurface with both phase and amplitude modulations, which consists of an artificially constructed metal-insulator-metal structure and two-dimensional graphene material. Each meta-atom of the metasurface is divided into two sub-atoms, and the two sub-atoms can reflect terahertz waves with a phase difference of 180°. Meanwhile, the amplitude of the sub-atom can be effectively modulated or even switched off by applying different gate voltages to the graphene. By independently controlling the amplitude response of the two sub-atoms, the whole meta-atom can dynamically control both amplitude and phase responses of the cross-polarization waves. By carefully designing the coding patterns, the digital metasurface can control both beam direction and intensity, which may lead to various advanced applications in beam shaping, radar detection systems, and high-quality holography.

Keywords: digital coding metasurface, programmable metasurface, graphene, amplitude modulation, phase modulation, terahertz beam manipulation

INTRODUCTION

Since 2014, the concept of digital coding metasurfaces and programmable metasurfaces has attracted growing interests (Cui et al., 2014). By binary encoding the meta-atoms' states of metasurfaces, the electromagnetic (EM) responses of meta-atoms can be characterized with n-bit digital code rather than continuous EM parameters, which built a bridge between the physical and digital world, and brought a new perspective of information science on metasurfaces (Cui et al., 2017; Cui et al., 2020). Metasurfaces or two-dimensional metamaterials have demonstrated unprecedented EM control capabilities in both scientific and engineering communities for their unique, finely tailorable properties (Zheludev and Kivshar, 2012; Wang et al., 2019; Fu et al., 2020). With superior capabilities in manipulating EM waves, metasurfaces have shown great flexibility in amplitude modulations, phase shifts, and polarization conversions (Yang et al., 2019; Shi et al., 2020; Wan et al., 2021). Owing to these unprecedented superiorities, many applications have been implemented such as beam steering, holograms, multiple beams, vortex beams, and so on (Yang et al., 2018b; Bodehou et al., 2020; Wang et al., 2020; Liu et al., 2021).

Until now, most metasurfaces focus on one of the three field: phase modulation, amplitude modulation, and polarization modulation, which cannot manipulate the EM waves comprehensively (Sun et al., 2020; Huang et al., 2021; Qing et al., 2021). Only a small number of cases of metasurfaces with both amplitude and phase modulations have been reported. In 2014, a transmissive metasurface with simultaneous control of phase and amplitude is proposed (Liu et al., 2014). The phase control is determined by the geometrical configuration of each meta-atom, and the amplitude control is realized by angular orientation manipulation. In 2018, a holographic metasurface with X-shaped meta-atoms is reported, which can control both phase and amplitude response by tuning the orientations of two arms (Lee et al., 2018). In 2019, Bao et al. proposed a method to form and control multiple beams independently, which requires both amplitude and phase control (Bao et al., 2019).

However, the cases mentioned above are all focused on passive devices, whose applications are limited by their fixed structures with single functionality. Thus, researchers look forward to finding active methods to manipulate both amplitude and phase in real-time. In 2022, Wang et al. demonstrated an intelligent metasurface with a three-ring structure. One out spilt ring provide the phase profile while the other two closed rings are used to control the amplitude response, and three varactor diodes are loaded in each meta-atoms to ensure active manipulating of both amplitude and phase response (Wang et al., 2022). However, in the terahertz (THz) band, the application of semiconductor components faces certain challenges, such as microelectromechanical system switches, and tunable materials, such as graphene, liquid crystals, and vanadium dioxide (Yang et al., 2018a; Ding et al., 2018; Roy et al., 2018; Zhang Zhang et al., 2018).

Graphene has been extensively demonstrated as an important tunable materials. Compare to other tunable materials like liquid crystals or barium strontium titanate, graphene can modulate conductivity rather than dielectric constant, which will benefit the independent modulation of amplitude and phase. Additionally, graphene can be controlled by an external electric field. Unlike other methods such as thermal or optical control, electrical control is preferred for its high efficiency, high speed, and compatibility with the circuit.

In this study, we propose a graphene-based programmable metasurface with both amplitude and phase modulations. The metasurface consists of an artificially constructed metal-insulator-metal structure and two-dimensional graphene material. The meta-atoms of the designed metasurface comprise two double-sided-arrow-shaped sub-atoms, and the two sub-atoms can reflect THz waves with a phase difference of 180°. The active electronically control of metasurface is enabled by integrating a single layer of graphene onto the metasurface. By applying different gate voltages to the graphene, the sub-atom will reflect the cross-polarized EM waves with different amplitudes or even switched off the cross-polarized reflected wave. By selecting one sub-atom to switch on and switching off the other sub-atom, the phase response of the meta-atom can be effectively modulated. We believe the designed THz digital programmable metasurface with the ability to control amplitude and phase responses independently has potential applications in beam shaping, radar detection systems, high-quality holography, and communication system.

GRAPHENE MODELING

Graphene, which is made up of a single layer of honeycomb-shaped carbon atoms, has been demonstrated as a promising platform for active reconfigurable THz devices for its high electrical tenability (Engel et al., 2018). To realize the precise evaluation of the modulated performance of the designed THz programmable metasurface, the graphene is modeled as an infinitesimally thin sheet. The surface conductivity of graphene consists of two components: the interband conductivity and the intraband conductivity (Zhang Zhang et al., 2018). According to the Pauli Exclusion Principle, the contribution of interband transitions is negligible in the THz band, and the Drude model of graphene surface conductivity in intraband can be described by (Wang et al., 2015):
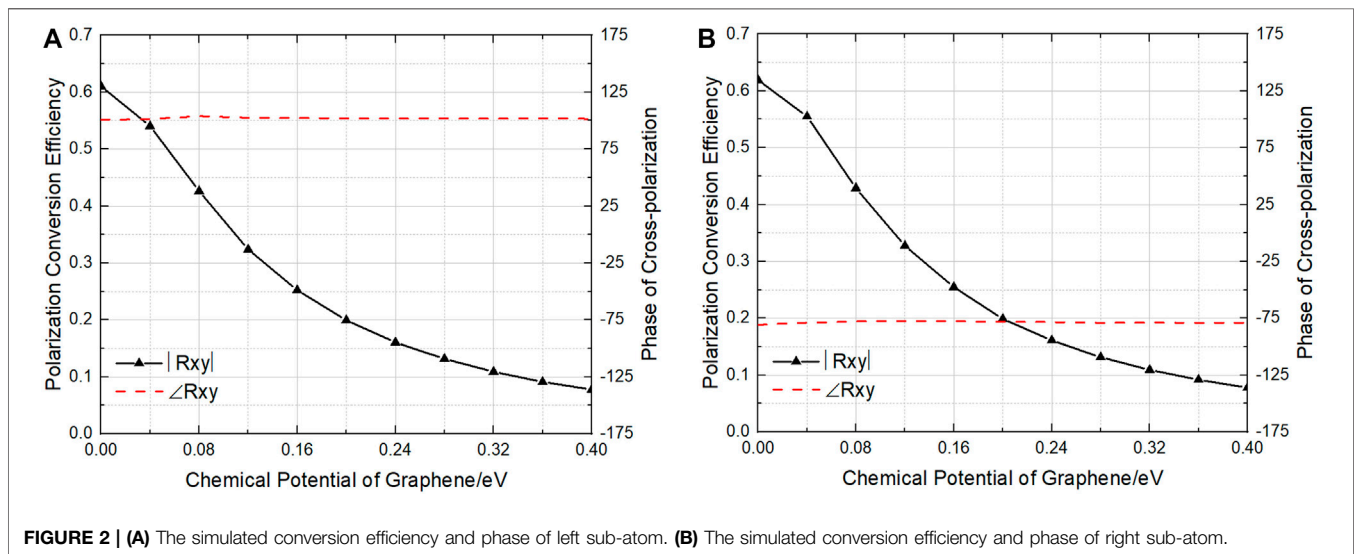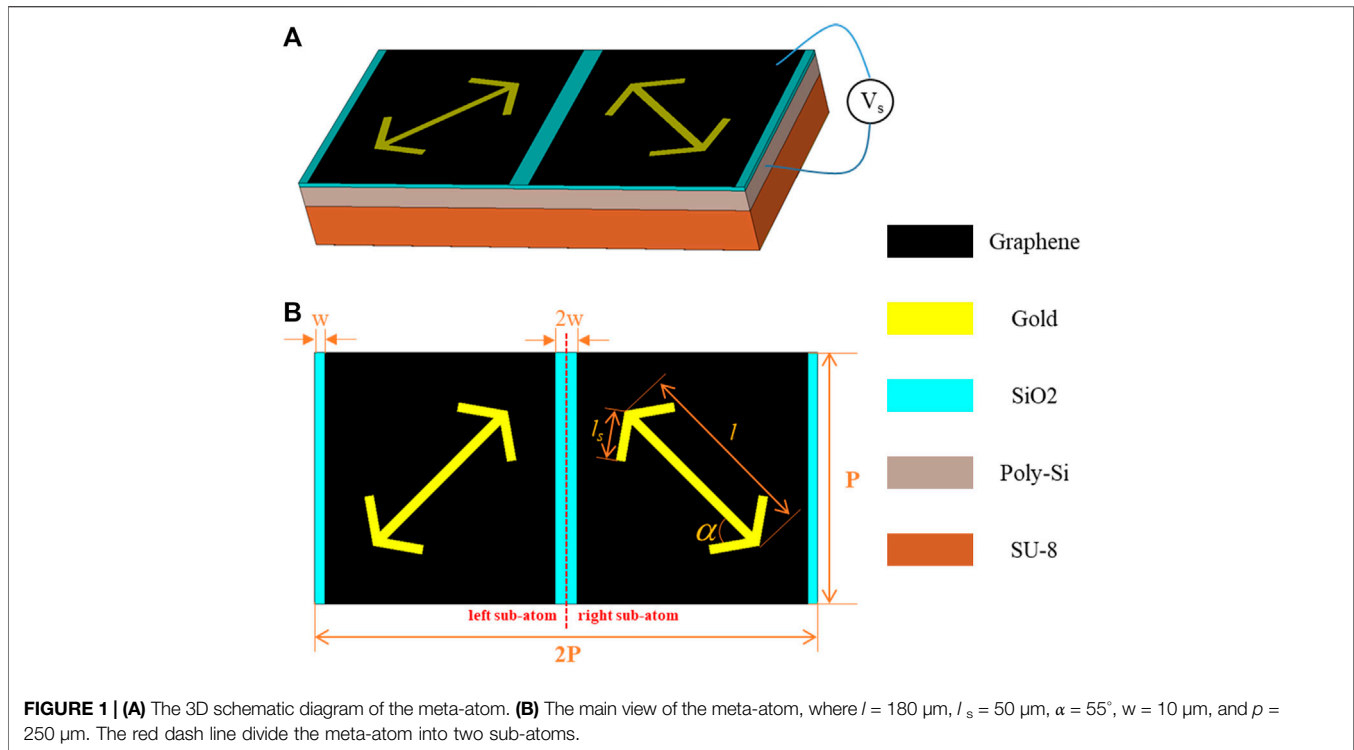
$$\sigma_s = \frac{e^2 k_B T \tau}{(1 + j\omega\tau)\pi\hbar^2} \left[\frac{\mu_c}{k_B T} + 2ln\left(e^{-\frac{\mu_c}{k_B T}} + 1 \right) \right] \tag{1}$$

where k_B is the Boltzmann constant, $\hbar$ is the reduced Plank constant, T is the temperature, ω is the angular frequency, e is the charge of the electron, τ is the relaxation time, and μ_c is the chemical potential of graphene. We assume T = 300 K and τ = 0.1 ps according to some practical works (Lee et al., 2012; Lee et al., 2018). Since the chemical potential of graphene μ_c can be effectively controlled by carrier concentration, the surface conductivity of graphene sheet can be modulated by external electric field. Hence, the EM response of the graphene metasurface can be electronically controlled.

DESIGN AND SIMULATION OF META-ATOMS

The 3D schematic and profile of the designed graphene-based meta-atom are shown in **Figure 1**. It consist of two sub-atoms with two mono-layer graphene patches under two double-sided-arrow-shaped metal patterns. The material SU-8 with 50 μm thickness sever as substrate, and a metal layer at the bottom sever as the ground. Above the substrate, a 25-μm-thick poly-silicon and a 300-nm-thick silicon oxide are used to change the chemical potential of the graphene. By applying different voltages between the graphene and the silicon, the chemical potential is changed, and the surface conductivity of graphene is effectively modulated.

As shown in **Figures 1A,B**, each meta-atom can be divided into two sub-atoms, and each sub-atom consists of a double-sided-arrow-shaped metal and a mono-layer graphene patch. The double-sided-arrow structure can realize the linear polarization conversion. The reflection magnitude of the cross-polarization under y-polarization incidence is simulated using CST

FIGURE 1 | (A) The 3D schematic diagram of the meta-atom. **(B)** The main view of the meta-atom, where $l = 180\ \mu m$, $l_s = 50\ \mu m$, $\alpha = 55°$, w = 10 μm, and $p = 250\ \mu m$. The red dash line divide the meta-atom into two sub-atoms.

FIGURE 2 | (A) The simulated conversion efficiency and phase of left sub-atom. **(B)** The simulated conversion efficiency and phase of right sub-atom.

Microwave Studio (3DS, France). After careful optimization, the designed parameters of the meta-atoms are $l = 180\ \mu m$, $l_s = 50\ \mu m$, $\alpha = 55°$, w = 10 μm, and $p = 250\ \mu m$. **Figure 2** is the simulated conversion efficiency and phase of each sub-atom. As we can see, with the increase of the chemical potential, the efficiency of polarization conversion decreases, The amplitude of cross-polarization reflect waves is close to 0 when the chemical potential of graphene is 0.4 eV, which can be regarded as the switched-off state. Correspondingly, when the chemical potential of graphene is lower than 0.4 eV, the states can be viewed as

switched on. The maximum conversion efficiency of each sub-atom is only 62%, which can be attributed to direct reflect from the graphene layer. Graphene has similar electromagnetic properties to metals, so most of the other energy is reflected in co-polarization. Meanwhile, the cross-polarization phase difference between the two sub-atoms is about 180°, and this difference can be attributed to the symmetry between the two sub-atoms.

The simulated cross-polarization response of the whole meta-atoms for different chemical potential at 0.45 THz is
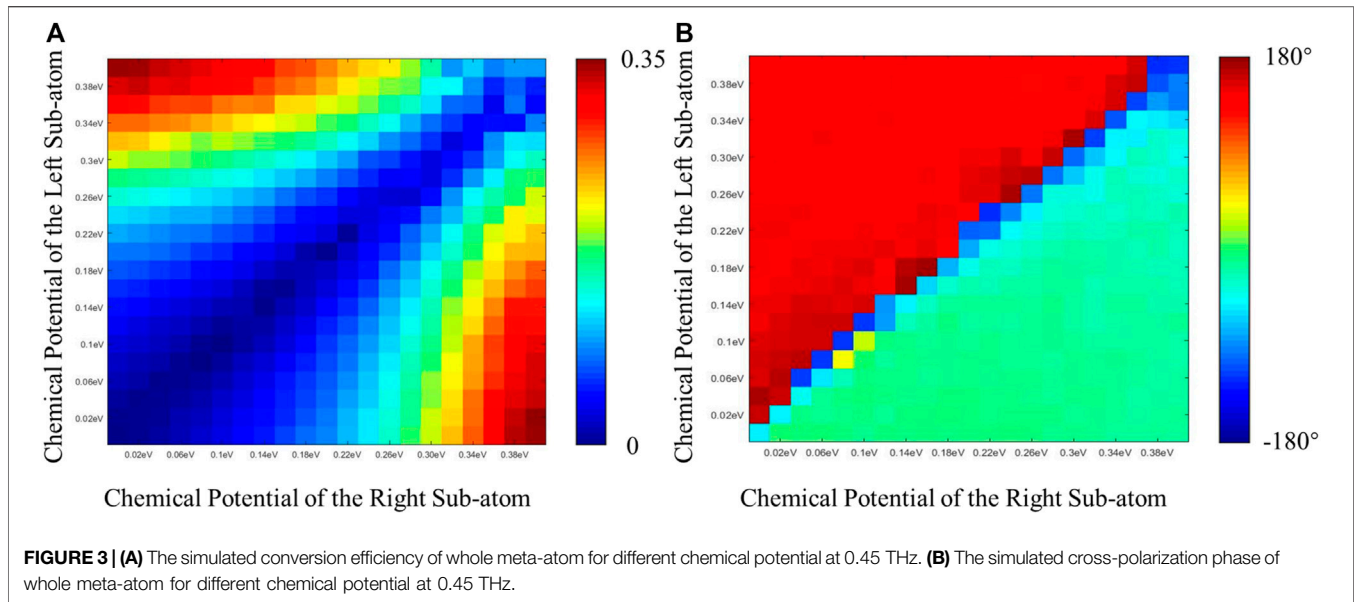
FIGURE 3 | (A) The simulated conversion efficiency of whole meta-atom for different chemical potential at 0.45 THz. (B) The simulated cross-polarization phase of whole meta-atom for different chemical potential at 0.45 THz.

TABLE 1 | The chemical potential of the left sub-atom and right sub-atom for different codes.

Codes	Chemical potential of the left sub-atom (eV)	Chemical potential of the right sub-atom (eV)
"11/1"	0.4	0.01
"11/0"	0.01	0.4
"10/1"	0.4	0.08
"10/0"	0.08	0.4
"01/1"	0.4	0.18
"01/0"	0.18	0.4
"00/1"	0.4	0.4
"00/0"	0.4	0.4

demonstrated on **Figure 3**. As we can see, the amplitude response can be modulated by changing the graphene chemical potential of the switched on sub-atom. Since the phase responses of the two sub-atoms are opposite, the reflected waves will cancel each other out, and the maximum amplitude can only be achieved when one of the sub-atom is switched off. Therefore, the amplitude response of meta-atoms can't exceed 50%. According to the simulation results, the amplitude response varies from 0.004 to 0.33, which means the amplitude modulation depth of the meta-atoms is about 98.8%. The minimum polarization conversion efficiency is much lower than single sub-atoms, which can also be attributed to the fact that the cross-polarization reflections of the two sub-atoms cancel each other out. In addition, the phase response of the meta-atoms can be controlled by choosing which sub-atoms is switched on, and the range of phase modulation is about 180°. Therefore, the phase responses of the meta-atoms meet the requirement of a 1-bit digital metasurface.
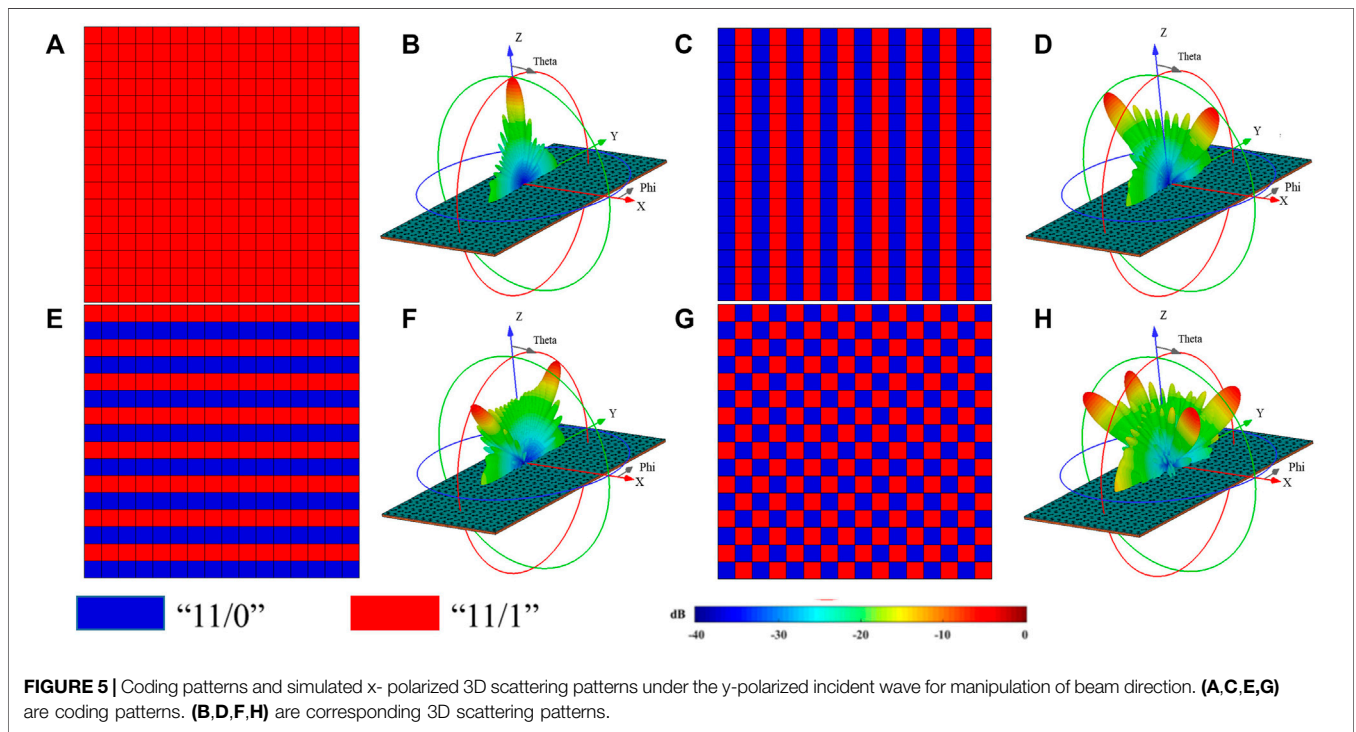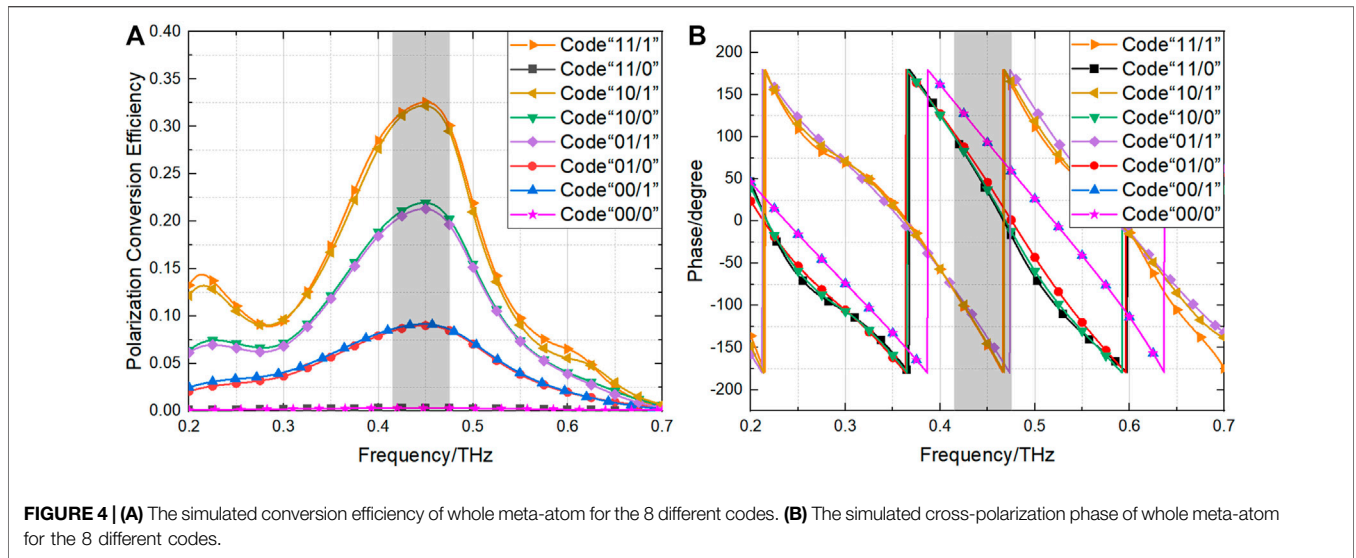
According to the simulated results, the state of the meta-atom are quantized to 8 codes, in which the amplitude response is 2 bits and the phase response is 1 bit. **Table 1** is the chemical potential of the left

sub-atom and right sub-atom for different amplitude and phase codes, and **Figure 4** is the simulated cross-polarization response for all 8 codes. The amplitude code "00", "01", "10" and "11" repentant 0, 11, 22 and 33% polarization conversion efficiency at 0.45THz, respectively. The phase code "0" and "1" repentant the 0 and 180° phase response, respectively. The codes of the whole meta-atom can be written in the form of "amplitude coding/phase coding". For the code "00/0" and "00/1", the two sub-atoms are both switched off, so their responses are actually the same. Considering the polarization conversion efficiency of the two coding states are 0, their phase responses is not important and can be ignored. As the **Figure 4** shows, the other 6 codes' phase responses and all 8 codes' amplitude responses are in good agreement with the design. The bandwidth of the metasurface is about 60 GHz (0.415THz-0.475 THz), which can be further extend by modifying the metal structures (Guo et al., 2020).

DESIGN OF CODING PATTERN

To demonstrate the powerful ability to modulate both amplitude and phase. We designed different coding pattern for the proposed metasurface that is composed of 16×16 sub-wavelength meta-atoms, and verified the ability to control the intensity and direction of the reflective beams. To simplifier the design process, we use the phase codes is designed to control the direction of the beams, while the amplitude codes to manipulate the intensity of the reflective beams. For the 1-bit digital metasurface, if the number of the meta-atoms is finite, and the codes of meta-atoms are arranged periodically, the maximum reflective intensity will be achieved, when and only when the elevation angle θ and azimuth angle φ satisfy the following equations (Xin Ge Zhang et al., 2018):

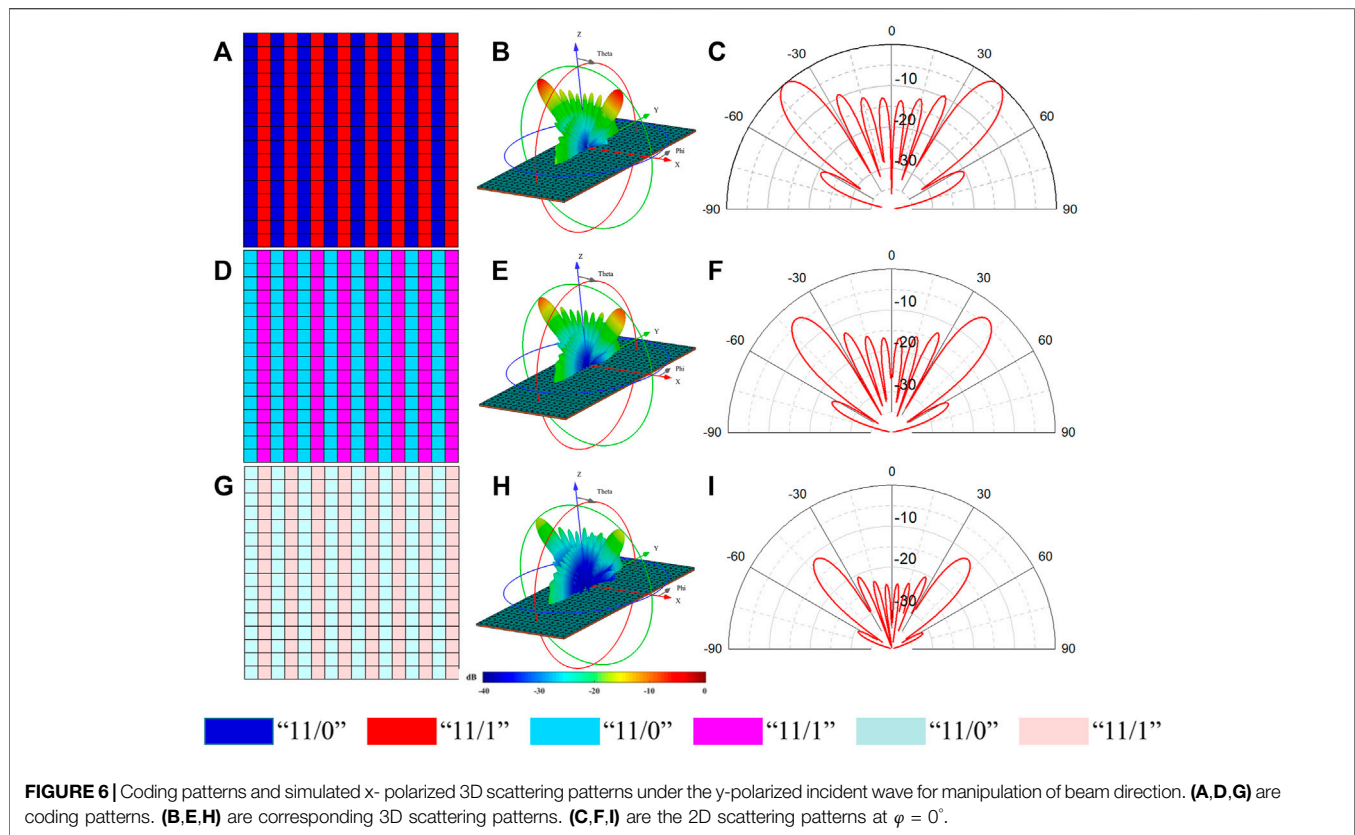$$\varphi = \pm \arctan\frac{\Gamma_x}{\Gamma_y}, \varphi = \pi \pm \arctan\frac{\Gamma_x}{\Gamma_y} \qquad (2)$$

FIGURE 4 | (A) The simulated conversion efficiency of whole meta-atom for the 8 different codes. **(B)** The simulated cross-polarization phase of whole meta-atom for the 8 different codes.

FIGURE 5 | Coding patterns and simulated x- polarized 3D scattering patterns under the y-polarized incident wave for manipulation of beam direction. **(A,C,E,G)** are coding patterns. **(B,D,F,H)** are corresponding 3D scattering patterns.

$$\theta = \arcsin\left(\lambda\sqrt{\frac{1}{\Gamma_x^2} + \frac{1}{\Gamma_y^2}}\right) \qquad (3)$$

where Γ_x and Γ_y are the physical periodic lengths of the coding sequence along the x- and y-directions, respectively. According to **Eqs 2**, **3**, the direction of the reflective beams mainly depends on the physical periodic lengths of the phase coding pattern.

The designed coding patterns and their corresponding simulated results at 0.45 THz are shown in **Figure 5**. At the working frequency 0.41THz, the transmitted beam is steered as the periodicity of the metasurface changes. For **Figure 5A**, all the meta-atoms' phase codes

are "0", which means the physical periodic lengths of the coding sequence is infinity in both the x- and y-directions, i.e., $\Gamma_x \rightarrow \infty$ and $\Gamma_y \rightarrow \infty$, so there is only one beam at $\theta = 0°$ (as the **Figure 5B** shows). For the **Figure 5C**, the physical periodic lengths of the coding sequence is $\Gamma_x = 4p = 1.5\lambda$ and $\Gamma_y \rightarrow \infty$, so the direction of the simulated beams (θ, φ) are (41°, 0°) and (41°, 180°). For the **Figure 5E**, $\Gamma_y = 8P = 3\lambda$ and $\Gamma_x \rightarrow \infty$, and the two main reflection beams are generated at (19.5°, 90°) and (19.5°, 270°), respectively (as the **Figure 5F** shows). For the **Figure 5G**, the phase codes changes in both x- and y-directions, and $\Gamma_x = 4p = 1.5\lambda$, $\Gamma_y = 8P = 3\lambda$. According to **Eq. 2** and **Eq. 3**, we will obtain four

FIGURE 6 | Coding patterns and simulated x- polarized 3D scattering patterns under the y-polarized incident wave for manipulation of beam direction. **(A,D,G)** are coding patterns. **(B,E,H)** are corresponding 3D scattering patterns. **(C,F,I)** are the 2D scattering patterns at $\varphi = 0°$.

main beams, and the direction of the four beams are (48.2°, 26.57°), (48.2°, -26.57°), (48.2°, 206.57°) and (48.2°, -206.57°) (as the **Figure 5H** shows). The simulated results demonstrated the proposed metasurface shows great ability of beam steering.

Next, we will verified the ability to control the intensity by changing the amplitude codes. In **Figure 5**, the amplitude codes of all meta-atoms are "11". In order to uniformly manipulate the intensity of all the outgoing beams, amplitude codes of all meta-atoms in **Figure 5C** are uniformly changed to "10" and "01" respectively, as the **Figures 6D,G** show. **Figures 6A,B** are the copy of the **Figures 5C,D**. The simulated results are demonstrated in **Figures 6E,H**, the intensity of the outgoing beams is reduced to −3.68 dB and −11.3 dB, respectively. **Figures 6C,F,I** are the 2D scattering patterns of **Figures 6B,E,H** at φ = 0°. The direction of the main beams are (41°, 0°) and (41°, 180°), which are same as the result in **Figure 5D**. Therefore, the modulation of amplitude and phase can is independent of each other.

CONCLUSION

In summary, we designed and simulated a graphene-based THz programmable digital-coding metasurface. The metasurface can actively manipulate both amplitude and phase response of cross-polarized reflected waves by controlling the graphene conductivity. The amplitude modulation depth of the meta-atoms is about 98.8%, while the phase-tuning range is 180°. On this basis, we designed the

coding patterns of the digital metasurface, and the metasurface successfully controls the beam direction and intensity. The simulated results demonstrate the designed graphene-based digital programmable metasurface has unprecedented capabilities to control and modulate THz beams. The designed digital programmable metasurfaces are expected to expand the potential applications for radar, sensing, and THz wireless communications.

DATA AVAILABILITY STATEMENT

The original contributions presented in the study are included in the article/Supplementary Material, further inquiries can be directed to the corresponding author.

AUTHOR CONTRIBUTIONS

CL and FY conceived the idea. FY supervised the theory. XF, JW, and LZ helped with the theoretical analyses. CL performed the theoretical calculations and all the simulations. CL and FY prepared the manuscript. All authors fully contribute to the research.

FUNDING

REFERENCES

Bao, L., Wu, R. Y., Fu, X., Ma, Q., Bai, G. D., Mu, J., et al. (2019). Multi-Beam Forming and Controls by Metasurface with Phase and Amplitude Modulations. *IEEE Trans. Antennas Propagat.* 67, 6680–6685. doi:10.1109/TAP.2019.2925289

Bodehou, M., Martini, E., Maci, S., Huynen, I., and Craeye, C. (2020). Multibeam and Beam Scanning with Modulated Metasurfaces. *IEEE Trans. Antennas Propagat.* 68, 1273–1281. doi:10.1109/TAP.2019.2944554

Cui, T. J., Qi, M. Q., Wan, X., Zhao, J., and Cheng, Q. (2014). Coding Metamaterials, Digital Metamaterials and Programmable Metamaterials. *Light Sci. Appl.* 3, e218. doi:10.1038/lsa.2014.99

Cui, T. J., Liu, S., and Zhang, L. (2017). Information Metamaterials and Metasurfaces. *J. Mat. Chem. C* 5, 3644–3668. doi:10.1039/C7TC00548B

Cui, T. J., Li, L., Liu, S., Ma, Q., Zhang, L., Wan, X., et al. (2020). Information Metamaterial Systems. *iScience* 23, 101403. doi:10.1016/j.isci.2020.101403

Ding, F., Zhong, S., and Bozhevolnyi, S. I. (2018). Vanadium Dioxide Integrated Metasurfaces with Switchable Functionalities at Terahertz Frequencies. *Adv. Opt. Mater.* 6, 1701204. doi:10.1002/adom.201701204

Engel, M., Farmer, D. B., Azpiroz, J. T., Seo, J.-W. T., Kang, J., Avouris, P., et al. (2018). Graphene-enabled and Directed Nanomaterial Placement from Solution for Large-Scale Device Integration. *Nat. Commun.* 9, 4095. doi:10.1038/s41467-018-06604-4

Fu, X., Yang, F., Liu, C., Wu, X., and Cui, T. J. (2020). Terahertz Beam Steering Technologies: From Phased Arrays to Field-Programmable Metasurfaces. *Adv. Opt. Mat.* 8, 1900628. doi:10.1002/adom.201900628

Guo, W. L., Wang, G. M., Luo, X. Y., Hou, H. S., Chen, K., and Feng, Y. (2020). Ultrawideband Spin-Decoupled Coding Metasurface for Independent Dual-Channel Wavefront Tailoring. *Ann. DER Phys.* 532, 1900472. doi:10.1002/andp.201900472

Huang, C. X., Zhang, J., Cheng, Q., and Cui, T. J. (2021). Polarization Modulation for Wireless Communications Based on Metasurfaces. *Adv. Funct. Mat.* 31, 2103379. doi:10.1002/adfm.202103379

Lee, S. H., Choi, M., Kim, T.-T., Lee, S., Liu, M., Yin, X., et al. (2012). Switching Terahertz Waves with Gate-Controlled Active Graphene Metamaterials. *Nat. Mater* 11, 936–941. doi:10.1038/nmat3433

Lee, G.-Y., Yoon, G., Lee, S.-Y., Yun, H., Cho, J., Lee, K., et al. (2018). Complete Amplitude and Phase Control of Light Using Broadband Holographic Metasurfaces. *Nanoscale* 10, 4237–4245. doi:10.1039/C7NR07154J

Liu, L., Zhang, X., Kenney, M., Su, X., Xu, N., Ouyang, C., et al. (2014). Broadband Metasurfaces with Simultaneous Control of Phase and Amplitude. *Adv. Mat.* 26, 5031–5036. doi:10.1002/adma.201401484

Liu, C. X., Yang, F., Fu, X. J., Wu, J. W., Zhang, L., Yang, J., et al. (2021). Programmable Manipulations of Terahertz Beams by Transmissive Digital Coding Metasurfaces Based on Liquid Crystals. *Adv. Opt. Mater.* 9, 2100932. doi:10.1002/adom.202100932

Qing, Y. M., Ma, H. F., and Cui, T. J. (2021). Multifunctional Space-Time-Coding Amplitude Modulated Graphene Metasurfaces. *J. Opt. Soc. Am. B* 38, 3206. doi:10.1364/JOSAB.435889

Roy, T., Zhang, S., Jung, I. W., Troccoli, M., Capasso, F., and Lopez, D. (2018). Dynamic Metasurface Lens Based on MEMS Technology. *Apl. Photonics* 3, 021302. doi:10.1063/1.5018865

Shi, Z., Zhu, A. Y., Li, Z., Huang, Y.-W., Chen, W. T., Qiu, C.-W., et al. (2020). Continuous Angle-Tunable Birefringence with Freeform Metasurfaces for Arbitrary Polarization Conversion. *Sci. Adv.* 6, eaba3367. doi:10.1126/sciadv.aba3367

Sun, Y.-L., Zhang, X.-G., Yu, Q., Jiang, W.-X., and Cui, T.-J. (2020). Infrared-controlled Programmable Metasurface. *Sci. Bull.* 65, 883–888. doi:10.1016/j.scib.2020.03.016

Wan, X., Xiao, Q., Zhang, Y. Z., Li, Y., Eisenbeis, J., Wang, J. W., et al. (2021). Reconfigurable Sum and Difference Beams Based on A Binary Programmable Metasurface. *Antennas Wirel. Propag. Lett.* 20, 381–385. doi:10.1109/LAWP.2021.3050808

Wang, X.-C., Zhao, W.-S., Hu, J., and Yin, W.-Y. (2015). Reconfigurable Terahertz Leaky-Wave Antenna Using Graphene-Based High-Impedance Surface. *IEEE Trans. Nanotechnol.* 14, 62–69. doi:10.1109/TNANO.2014.2365205

Wang, L., Zhang, Y., Guo, X., Chen, T., Liang, H., Hao, X., et al. (2019). A Review of THz Modulators with Dynamic Tunable Metasurfaces. *Nanomaterials* 9, 965. doi:10.3390/nano9070965

Wang, Z. X., Wu, J. W., Wu, L. W., Gou, Y., Ma, H. F., Cheng, Q., et al. (2020). High Efficiency Polarization-Encoded Holograms with Ultrathin Bilayer Spin-Decoupled Information Metasurfaces. *Adv. Opt. Mat.* 9, 2001609. doi:10.1002/adom.202001609

Wang, H. P., Li, Y. B., Li, H., Shen, J. L., Dong, S. Y., Wang, S. Y., et al. (2022). Intelligent Metasurface with Frequency Recognition for Adaptive Manipulation of Electromagnetic Wave. *Nanophotonics* 11, 1401–1411. doi:10.1515/nanoph-2021-0799

Xin Ge Zhang, X. G., Tang, W. X., Jiang, W. X., Bai, G. D., Tang, J., Bai, L., et al. (2018). Light-Controllable Digital Coding Metasurfaces. *Adv. Sci.* 5, 1801028. doi:10.1002/advs.201801028

Yang, J., Cai, C., Yin, Z., Xia, T., Jing, S., Lu, H., et al. (2018a). Reflective Liquid Crystal Terahertz Phase Shifter with Tuning Range of over 360°. *IET Microwaves, Antennas & Propag.* 12, 1466–1469. doi:10.1049/iet-map.2017.0898

Yang, J., Zhang, C., Ma, H. F., Zhao, J., Dai, J. Y., Yuan, W., et al. (2018b). Generation of Radio Vortex Beams with Designable Polarization Using Anisotropic Frequency Selective Surface. *Appl. Phys. Lett.* 112, 203501. doi:10.1063/1.5029507

Yang, J., Wang, P., Shi, T., Gao, S., Lu, H., Yin, Z., et al. (2019). Electrically Tunable Liquid Crystal Terahertz Device Based on Double-Layer Plasmonic Metamaterial. *Opt. Express* 27, 27039. doi:10.1364/OE.27.027039

Zhang Zhang, Z., Yan, X., Liang, L., Wei, D., Wang, M., Wang, Y., et al. (2018). The Novel Hybrid Metal-Graphene Metasurfaces for Broadband Focusing and Beam-Steering in Farfield at the Terahertz Frequencies. *Carbon* 132, 529–538. doi:10.1016/j.carbon.2018.02.095

Zheludev, N. I., and Kivshar, Y. S. (2012). From Metamaterials to Metadevices. *Nat. Mater* 11, 917–924. doi:10.1038/nmat3431